Proof of concept for a nonadditive stochastic model of supercooled liquids

A. C. P. Rosa, Jr., E. Brito, W. S. Santana, and C. Cruz*
Centro de Ciências Exatas e das Tecnologias, Universidade Federal do Oeste da Bahia, Rua Bertioga, 892 Morada Nobre I, 47810-059 Barreiras, Bahia, Brazil

(Received 16 March 2024; accepted 10 June 2024; published 19 July 2024)

The recently proposed nonadditive stochastic model (NSM) offers a coherent physical interpretation for diffusive phenomena in glass-forming systems. This model presents nonexponential relationships between viscosity, activation energy, and temperature, characterizing the non-Arrhenius behavior observed in supercooled liquids. In this work, we fit the NSM viscosity equation to experimental temperature-dependent viscosity data corresponding to 25 glass-forming liquids and compare the fit parameters with those obtained using the Vogel-Fulcher-Tammann (VFT), Avramov-Milchev (AM), and Mauro-Yue-Ellison-Gupta-Allan (MYEGA) models. The results demonstrate that the NSM provides an effective fitting equation for modeling viscosity experimental data in comparison with other established models (VFT, AM, and MYEGA), characterizing the activation energy in fragile liquids, presenting a reliable indicator of the degree of fragility of the glass-forming liquids.

DOI: 10.1103/PhysRevE.110.014128

I. INTRODUCTION

Glass science is a developing field of research due to the numerous technological applications of glass-forming liquids, and the formation mechanisms of amorphous solids remain an open question in the literature [1–5]. The glass-forming process involves a liquid cooling to below its melting temperature without crystallizing, resulting in a metastable state called supercooled liquid. As the supercooled liquid cools, it becomes highly viscous until it passes through the glass transition, resulting in an amorphous solid structure [1,5,6]. Intermolecular bonds in the supercooled liquid impose a potential barrier to viscous flow, i.e., viscosity is a thermally activated quantity, and its activation energy depends on temperature for several substances. In this scenario, glass-forming liquids can be classified into two categories [4,6]: *strong liquids*, which increase viscosity exponentially with temperature [7], and *fragile liquids*, which have nonexponential viscosity curves [4,6–8].

To get a satisfactory interpretation of the non-Arrhenius behavior in supercooled liquids, the authors of this paper developed the so-called nonadditive stochastic model (NSM) for the study of the reaction-diffusion processes in supercooled liquids [4]. For the NSM, due to the dissipative effects present in the supercooled liquid during the diffusion process, the fluid concentration obeys a nonhomogeneous continuity equation, and these correspond to a nonlinear Fokker-Planck equation [4]. This proposed approach provides nonexponential functions for the thermal behavior of viscosity and the activation energy in fragile liquids. In other recent work, the group analyzed the viscosity equation in fragile liquids from the NSM, focusing on the relationship between activation energy and temperature [5]. The findings show that the fragility index is directly proportional to the activation energy for the glass transition temperature. In this regard, the developed approach appears in the literature as a robust method to characterize the degree of fragility of glass-forming systems and establishes the fragility index as a function of a γ exponent [5,9–15].

In this context, this paper expands the previous research and serves as a proof-of-concept for the NSM in experimental settings. We analyze temperature-dependent viscosity data for 25 different glass-forming materials and use the NSM viscosity equation to determine the behavior of the activation energy with temperature. For each substance, we determine the glass transition temperature and the fragility index values. Additionally, we compare the NSM's fit parameters with those of other viscosity models such as the Vogel-Fulcher-Tammann (VFT), Avramov-Milchev (AM), and Mauro-Yue-Ellison-Gupta-Allan (MYEGA) models [16,17]. The results demonstrate that the NSM is more accurate than these models for studying temperature-dependent viscosity in glass-forming liquids that exhibit super-Arrhenius behavior. Thus, the NSM provides a solid way to physically interpret the formation mechanisms of amorphous solids.

II. VISCOSITY OF GLASS-FORMING SYSTEMS

Viscosity is the reciprocal of fluidity [4–6], and the latter emerges naturally from the generalized drag coefficient that compounds the continuity equation in the NSM formalism [4,5]. Usually, experimental viscosity data are in units of *Pa s* or *Poise*, and the values measured near the glass transition are very high in both units. Therefore, the logarithmic scale is the most efficient for representing experimental viscosity measurements. Thus, for the stationary regime of the reaction-diffusion process, the dependence of viscosity on temperature is characterized by a three-parameter model, written in the logarithmic scale as,

$$\log_{10}\eta(T) = \log_{10}(\eta_\infty) - \gamma\log_{10}\left[1 - \frac{T_t}{T}\right], \qquad (1)$$

where η_∞ is the high-temperature viscosity limit, T_t is the viscosity divergence threshold temperature, and γ is a

*Contact author: clebson.cruz@ufob.edu.br

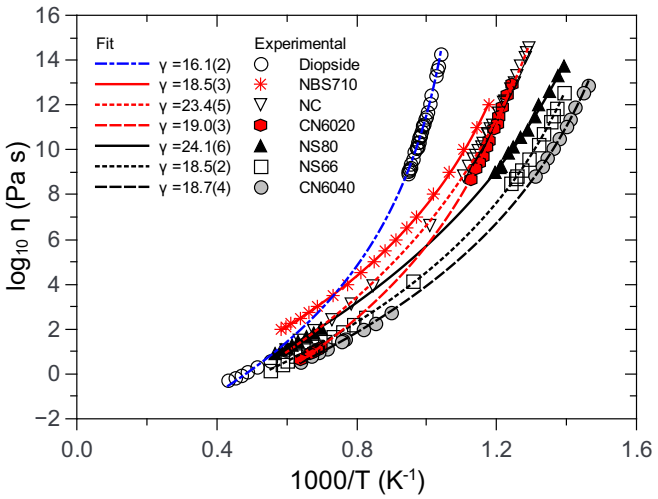

FIG. 1. Variation of the logarithm of viscosity as a function of the reciprocal temperature for silicate glasses [20–23]. The miscellaneous symbols corresponds to the experimental data, and the curve lines (continuous and dashed) to the fit of Eq. (1).

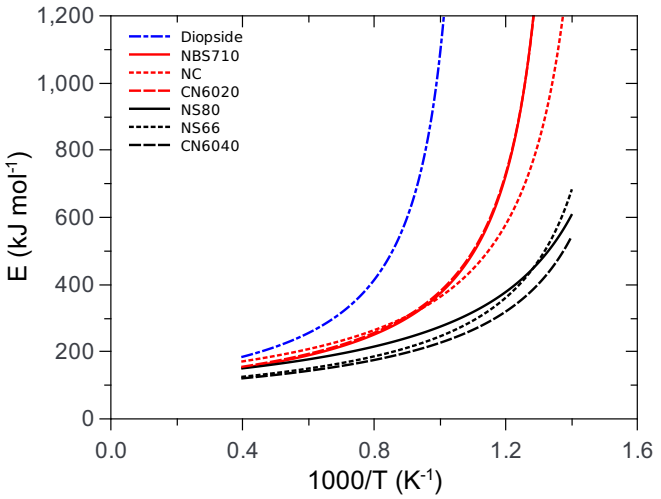

FIG. 2. Activation energy as a function of the reciprocal temperature using the fit parameters from Table I in Eq. (2). Curve lines (continuous and dashed) for silicate glasses.

characteristic exponent directly related to the fragility degree of the glass-forming liquid [5].

It is worth mentioning that, despite the similarity with the viscosity equation of other approaches, such as the mode-coupling theory (MCT), Eq. (1) does not diverge for the glass transition temperature (T_g), in contrast to a typical MCT prediction [18]. Furthermore, it is important to mention that Eq. (1) is consistent with the microscopic-phenomenological models of the glass transition [19]. Thus, the viscosity generated from the NSM exhibits consistent temperature-dependent behavior, suggesting that the NSM provides an accurate description of the glass transition phenomena, highlighting the potential of this model in capturing the complex dynamics of glassy materials. In this regard, this work validates the NSM by analyzing experimental temperature-dependent viscosity data from silicate glasses [20–23], borosilicates [24], aluminosilicates [20,21,25], titania silicates [26], and chalcogenide glasses [17,27–29], totaling 25 glass-forming materials.

Figure 1 shows the curves (continuous and dashed lines) corresponding to nonlinear regression fitting of the Eq. (1) for viscosity experimental data (miscellaneous symbols) of the silicate glasses – for other substances, see Fig. 5 in Appendix A. Table I (see Appendix A) contains the fit parameters obtained for all glass-forming substances. The Pearson coefficient R^2 values are on the order of 0.999, and the χ^2 test provides values below 0.1, demonstrating that Eq. (1) provides an excellent fit to the viscosity-temperature data. From the γ and T_t values in Table I, we calculated for all compositions the temperature-dependent activation energy, expressed by

$$E(T) = \frac{\gamma R}{\ln 10}\left(\frac{T_t}{1-\frac{T_t}{T}}\right), \tag{2}$$

where R is the universal gas constant. Figure 2 shows the super-Arrhenius behavior for silicate glasses–see Fig. 6 in Appendix A for the other substances. The activation energy is an increasing function of the reciprocal temperature, and $E(T)$ grows as it approaches the glass transition for all analyzed glass-forming materials. Considering the reference value 10^{12} *Pa s* for viscosity [6] in Eq. (1), we can estimate the glass transition temperature T_g, given by,

$$T_g = \frac{T_t}{1-10^{-B/\gamma}}, \tag{3}$$

where $B = 12 - \log\eta_\infty$. Table I (see Appendix A) contains the T_g values determined from Eq. (3) for all glass-forming substances.

Furthermore, the condition $T_t < T_g$ allows us to associate the viscosity divergence temperature in our model with the Kauzmann's temperature (T_K) for which the configurational entropy of the supercooled liquid vanishes, i.e., the entropy of the glass is equal to the entropy of the correspondent crystalline phase [30–32]. Below T_K, the supercooled liquid would have unrealistic physical behavior that violates the Third Law of Thermodynamics, defining the well-known Kauzmann paradox, an open question in glass science [30–32]. In a practical scenario, the glass-forming substance experiences both structural and dynamic changes when temperatures are near T_K (where $T_g < T < T_K$). This leads to a change in the generalized activation energy, denoted as E, Eq. (2), which defines the threshold temperature T_t [4,5]. As a result, the supercooled liquid state is unable to reach the condition of viscosity divergence. Thus, $T_t < T_k$; otherwise, it would never be reached. Conversely, it is important to note that delving into this topic is out of the scope of this paper. The NSM provides a reliable fragility index (M_η) directly proportional to $E(T_g)$ [5] and, from Eq. (1) and Eq. (2), we established one unique relation between the fragility index and the γ exponent [5], expressed as

$$M_\eta = \frac{\gamma}{\ln 10}\left(10^{B/\gamma} - 1\right). \tag{4}$$

The concept of fragility in glass science is related to the degree of short-range order of the atomic arrangement of the supercooled liquid upon cooling through the glass transition so that, unlike strong liquids, a well-defined short-range order is lacking in fragile liquids [17]. According to Eq. (4), the greater the slope of the activation energy curve as the

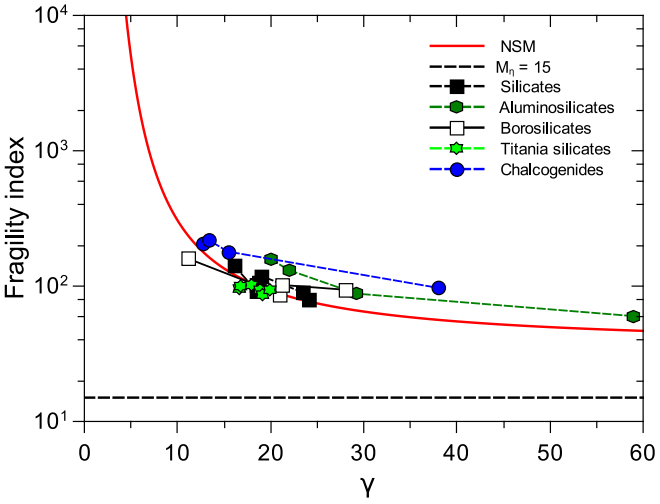

FIG. 3. The fragility index as a function of the exponent γ. The miscellaneous symbols correspond to the data in Table I, and the curve (red line) corresponds to the Eq. (3) for $B = 15$. The horizontal line (dashed line) corresponds to the value $M_\eta = 15$ and is an asymptotic limit between fragile and strong behaviors.

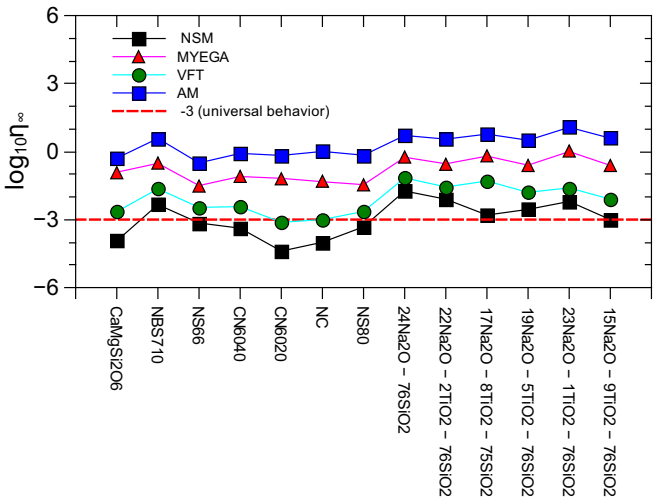

FIG. 4. The logarithm of the high-temperature viscosity limit for silicates [20–23] and titania silicates [26] glasses. The miscellaneous symbols correspond to the values of the $\log_{10}\eta_\infty$ obtained by the NSM (see Table I), AM, VFT, and MYEGA (see Table II) equations. The dashed red line corresponds to the universal behavior for η_∞.

substance approaches the glass transition, the greater the fragility index value, which implies a lower value for the respective γ exponent. Table I (see Appendix A) contains the M_η values determined from Eq. (4) for all glass-forming substances. Figure 3 shows the fragility index as a function of the γ exponent, where the miscellaneous symbols correspond to the data in Table I and the red line corresponds to Eq. (4) for $B = 15$ ($\log \eta_\infty \approx -3$) [5]. The dispersion of the data relative to the theoretical curve is due to the variability of the experimental values of $log\eta_\infty$ obtained for each glass-forming substance. The horizontal line (dashed line) corresponds to the asymptotic limit between fragile and strong liquids, valid from the $\gamma \to \infty$ condition, implying $M_\eta = B$.

III. VISCOSITY MODELS

We compare the NSM with the Vogel-Fulcher-Tammann (VFT), Avramov-Milchev (AM), and Mauro-Yue-Ellison-Gupta-Allan (MYEGA) models [16,17], which provide three efficient temperature-dependent viscosity equations to model non-Arrhenius behavior in supercooled liquids. Our objective is to conduct a comparative analysis of the accuracy of the NSM and other three-parameter equations for fitting experimental data. The analysis of the different theoretical interpretations of the other models is out of the scope of this paper and can be found in the specialized literature [16,17,33]. The VFT equation [17,33] can be described as,

$$\log_{10}\eta(T) = \log_{10}(\eta_\infty) + \frac{A}{T - T_0}, \tag{5}$$

where η_∞, B, and T_0 are the fitting parameters. In this case, A is an activation barrier, and T_0 is a viscosity divergence temperature. The AM model assumes that the structural disorder of the glass-forming liquid produces a random distribution of activation barriers whose dispersion around the mean activation energy depends on the system entropy [34]. The AM equation can be expressed as

$$\log_{10}\eta(T) = \log_{10}(\eta_\infty) + \left(\frac{\tau}{T}\right)^\alpha, \tag{6}$$

where η_∞, τ, and α are the fitting parameters. In this case, τ is a temperature associated with a reference entropy, and the exponent α is related to the fragility index that emerges from the AM model [17,34].

The MYEGA equation, which derives from the Adam-Gibbs model that relates viscosity to the configurational entropy of the supercooled liquid [16], is given by

$$\log_{10}\eta(T) = \log_{10}(\eta_\infty) + \frac{K}{T}\exp\left(\frac{C}{T}\right) \tag{7}$$

where η_∞, K, and C are the fitting parameters. In Eq. (7), the exponential function defines the configurational entropy of the supercooled liquid, and K is an effective activation barrier. According to Table II (see Appendix B), the values of χ^2 and R^2 obtained from the nonlinear fit of Eqs. (5), (6), and (7), about the experimental data of all analyzed glass-forming substances, are in the same order of magnitude as the values obtained from Eq. (1) for the same parameters. Therefore, the results demonstrate that the NSM provides as effective a fitting equation for modeling temperature-dependent viscosity experimental data as the VFT, AM, and MYEGA equations.

Table II contains the $\log_{10}\eta_\infty$ values obtained from the AM, VFT, and MYEGA models, given that the fit parameter is common to the four viscosity equations (see Table I for the corresponding values of the NSM). Experimental evidence indicates that the condition $\log_{10}\eta_\infty \approx -3$ is associated with universal behavior for the high-temperature viscosity limit [5,17], a result whose verification is beyond the scope of this work. Despite this, we can qualitatively discuss the results obtained for the high-temperature viscosity limit relative to the universal behavior mentioned above. Thus, Fig. 4 illustrates the dispersion of the $\log_{10}\eta_\infty$ fit values obtained by each of the four viscosity models (miscellaneous symbols) about the -3 reference value (red dashed line).

We considered only the silicate and titania-silicate glasses because the four viscosity equations provided less dispersed values for $\log_{10}\eta_\infty$ for these materials if compared to other

glass-forming liquids. The results demonstrated that the NSM provides η_∞ values close to the limit of 10^{-3} Pa s for silicate and titania-silica glasses, and other viscosity models tend to overestimate the high-temperature viscosity limit for the same substances, this behavior being more critical in the AM model.

IV. CONCLUSION

In summary, this work demonstrates a proof-of-concept for the NSM model in experimental settings. The results demonstrated that the NSM is efficient for characterizing the temperature-dependent viscosity of glass-forming liquids in which the activation energy varies with the temperature. The values of χ^2 and R^2 obtained from the nonlinear regression of Eq. (1) imply that the NSM accurately adjusted the experimental temperature-dependent viscosity data of the 25 glass-forming substances analyzed. These parameters are in the same order of magnitude if compared to values of the χ^2 and R^2 obtained by the VFT, AM, and MYEGA equations, widely used to model temperature-dependent viscosity in supercooled liquids. From the fit parameters of Eq. (1), we calculated the experimental values from the activation energy [see Eq. (2)] and the glass transition temperature [see Eq. (3)]. Also, we demonstrated the robustness of Eq. (4), which makes the exponent γ a reliable indicator of the degree of fragility of the glass-forming substance. Finally, we verified that, while the NSM provided values for the high-temperature viscosity limit close to the universal behavior 10^{-3} Pa s from the silicates and titania-silica glasses, the other viscosity models overestimate η_∞ for the same substances. Thus, the results demonstrate that the NSM guarantees a solid interpretation for diffusive processes in supercooled liquids that exhibit non-Arrhenius behavior and consolidates the NSM as a robust theoretical basis for the physical interpretation of the dynamic properties of glass-forming systems.

ACKNOWLEDGMENT

The authors thank the Fundação de Amparo à Pesquisa do Estado da Bahia–FAPESB for its financial support (Grant No. APP0041/2023).

APPENDIX A: FIT PARAMETERS OF THE NSM

Similar to Fig. 1, Fig. 5 shows the logarithm of viscosity as a function of the reciprocal temperature for other glass-forming substances, where the miscellaneous symbols are

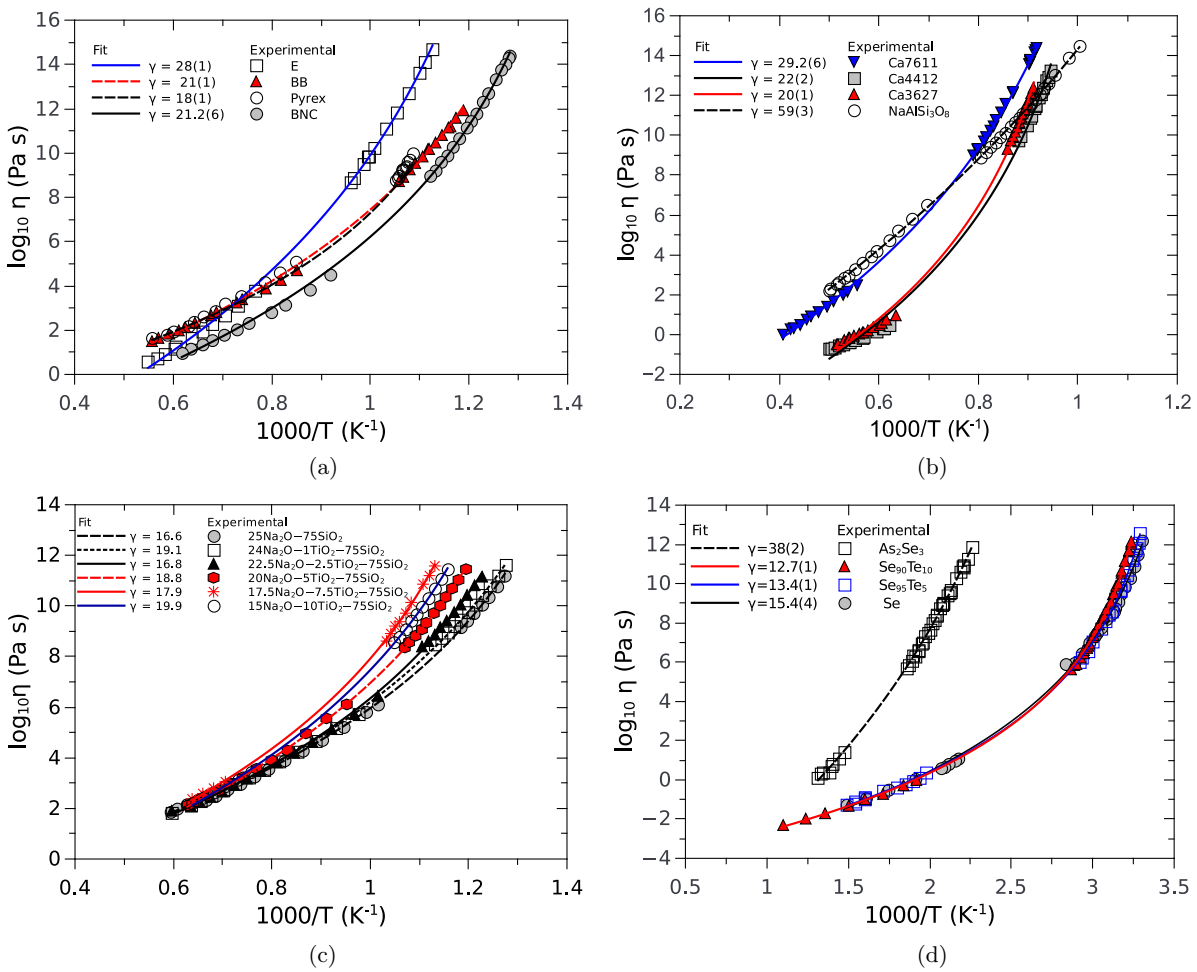

FIG. 5. Variation of the logarithm of viscosity as a function of the reciprocal temperature for glass-forming liquids. Experimental data (miscellaneous symbols): (a) borosilicates [24], (b) aluminosilicates [20,21,25], (c) titania silicates [26], and (d) chalcogenides [17,27–29] glasses. Curved lines (continuous and dashed): fit the Eq. (1) for (a) borosilicates, (b) aluminosilicates, (c) titania silicates, and (d) chalcogenides glasses.

TABLE I. Fit parameters of Eq. (1) for temperature-dependent viscosity data of 25 glass-forming liquids, including silicates [20–23], borosilicates [24], aluminosilicates [20,21,25], titania silicates [26], and chalcogenides [17,27–29] glasses. We calculated the T_g values by the Eq. (3) and the M_η values by the Eq. (4).

Glass	$\log_{10}\eta_\infty$	R^2	χ^2 ($\times 10^{-2}$)	γ	T_t (K)	T_g (K)	M_η
Silicates							
$CaMgSi_2O_6$	−3.94(7)	0.9994	1.1	16.1(2)	890(3)	991(22)	141(4)
NBS710	−2.34(5)	0.9999	0.1	18.5(3)	708(3)	851(23)	92(3)
NS66	−3.15(4)	0.9999	0.2	18.5(2)	615(2)	725(12)	103(2)
CN6040	−3.38(7)	0.9998	0.4	18.7(4)	593(4)	698(21)	106(4)
CN6020	−4.39(6)	0.9999	0.3	19.0(3)	706(3)	818(17)	119(3)
NC	−4.0(1)	0.9996	0.8	23.4(5)	651(4)	821(27)	90(4)
NS80	−3.32(8)	0.9998	0.5	24.1(6)	578(5)	752(27)	80(4)
Aluminosilicates							
Ca3627	−7.0(4)	0.9984	5.1	20(1)	980(20)	1104(87)	158(15)
Ca4412	−6.5(3)	0.9976	9.2	22(2)	950(10)	1110(114)	131(18)
Ca7611	−5.65(8)	0.9998	0.6	29.2(6)	867(6)	1154(30)	88(3)
$NaAlSi_3O_8$	−5.9(1)	0.9998	0.3	59(3)	550(10)	1094(62)	60(5)
Borosilicates							
Pyrex	−1.2(2)	0.9977	3.1	11.1(6)	832(8)	890(156)	160(30)
BB	−2.9(2)	0.9992	1.4	21(1)	680(12)	845(75)	87(9)
BNC	−4.2(1)	0.9994	1.6	21.2(6)	678(5)	819(31)	102(5)
E	−5.9(2)	0.9994	1.7	28(1)	725(9)	941(48)	94(6)
Titania-Silica							
$24Na_2O-76SiO_2$	−1.74(7)	0.9998	0.3	16.6(4)	655(6)	769(37)	95(5)
$22Na_2O-2TiO_2-76SiO_2$	−2.1(1)	0.9994	0.7	16.8(6)	685(7)	801(48)	99(7)
$17Na_2O-8TiO_2-75SiO_2$	−2.8(1)	0.9998	0.2	17.9(5)	743(6)	873(40)	102(6)
$19Na_2O-5TiO_2-76SiO_2$	−2.55(9)	0.9998	0.2	18.8(4)	687(5)	826(35)	93(4)
$23Na_2O-1TiO_2-76SiO_2$	−2.20(8)	0.9998	0.3	19.1(5)	638(6)	779(36)	87(5)
$15Na_2O-9TiO_2-76SiO_2$	−3.0(1)	0.9998	0.3	19.9(7)	703(8)	853(42)	93(6)
Chalcogenides							
$Se_{90}Te_{10}$	−3.7(1)	0.9996	0.7	12.7(1)	296.6(8)	315(9)	206(6)
$Se_{95}Te_5$	−4.75(5)	0.9998	0.7	13.4(1)	287.9(5)	306(4)	218(3)
Se	−5.0(1)	0.9988	2.4	15.4(4)	279(2)	303(10)	180(8)
As_2Se_3	−8.9(2)	0.9993	1.0	38(2)	318(6)	443(27)	97(8)

experimental viscosity data refer to (5a) borosilicates [24], (5b) aluminosilicates [20,21,25], (5c) titania silicates [26], and (5d) chalcogenides glasses. The continuous and dashed lines correspond to the nonlinear regression fitting of Eq. (1) using the Levenberg-Marquadt method [35] for all cases. Table I contains the fit parameters γ, $\log_{10}\eta_\infty$ and T_t from the Eq. (1), the Pearson coefficient R^2 and the χ^2 test obtained for all glass-forming substances analyzed. The fragility index values calculated by Eq. (3) and the glass transition temperature values by Eq. (4) complete Table I. We apply the error propagation method to determine the uncertainties about the M_η and T_g values. Similar to Fig. 2, Fig. 6 shows the activation energy as a function of the reciprocal temperature for (6a) borosilicates, (6b) aluminosilicates, (6c) titania silicates, and (6d) chalcogenides glasses. Curve lines (continuous and dashed) correspond to Eq. (2) using the fit parameters from Table I.

APPENDIX B: FIT PARAMATERS OF THE AM, VFT, AND MYEGA MODELS

Table II list the values of $\log_{10}\eta_\infty$, R^2, and χ^2 obtained from the nonlinear regression fitting of the Eq. (5) (VFT), Eq. (6) (AM), and Eq. (7) (MYEGA) using the Levenberg-Marquadt method [35] for experimental temperature-dependent viscosity data of the 25 glass-forming liquids analyzed in this work.

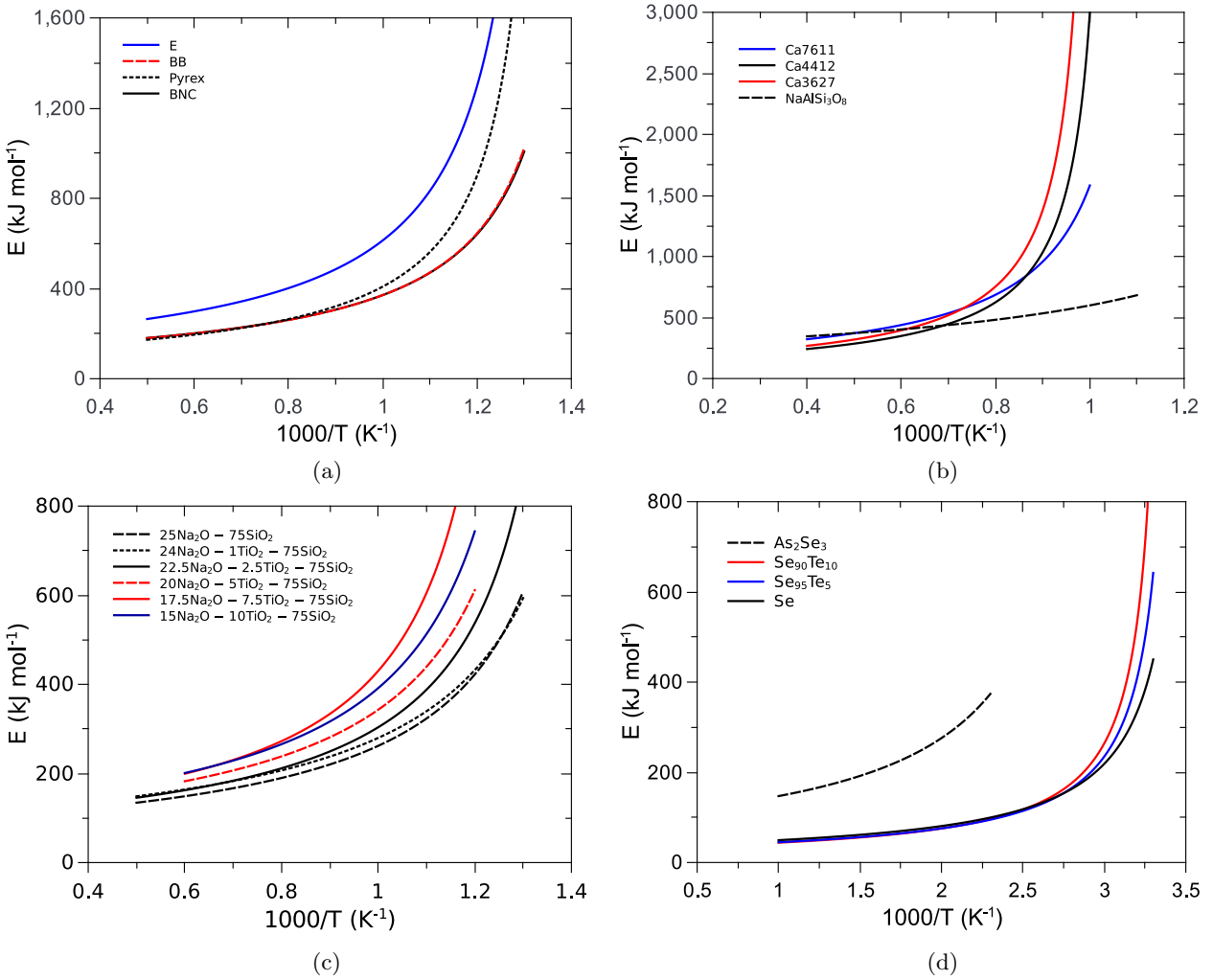

FIG. 6. Activation energy as a function of the reciprocal temperature using the fit parameters from Table I in Eq. (2). Curved lines (continuous and dashed) for (a) silicates, (b) borosilicates, (c) aluminosilicates, (d) titania silicates, and (e) chalcogenides glasses.

TABLE II. $\log_{10}\eta_\infty$, R^2, and χ^2 obtained from AM, VFT, and MYEGA equations for temperature-dependent viscosity data of 25 glass-forming liquids, including silicates [20–23], borosilicates [24], aluminosilicates [20,21,25], titania silicates [26], and chalcogenides [17,27–29] glasses.

Glass	AM $\log_{10}\eta_\infty$	AM R^2	AM χ^2 ($\times10^{-2}$)	VFT $\log_{10}\eta_\infty$	VFT R^2	VFT χ^2 ($\times10^{-2}$)	MYEGA $\log_{10}\eta_\infty$	MYEGA R^2	MYEGA χ^2 ($\times10^{-2}$)
Silicates									
$CaMgSi_2O_6$	−0.29(4)	0.9996	0.8	−2.65(4)	0.9999	0.3	−0.91(3)	0.9999	0.3
NBS710	0.58(8)	0.9997	0.3	−1.642(7)	0.99999	0.002	−0.52(6)	0.9999	0.1
NS66	−0.5(2)	0.9988	2.7	−2.46(8)	0.9998	0.5	−1.5(2)	0.9993	1.5
CN6040	−0.08(14)	0.9994	1.6	−2.43(6)	0.9999	0.2	−1.1(1)	0.9997	0.7
CN6020	−0.17(4)	0.99993	0.2	−3.12(5)	0.9999	0.1	−1.18(5)	0.99996	0.1
NC	0.007(72)	0.9998	0.4	−3.00(7)	0.9998	0.3	−1.33(6)	0.9999	0.2
NS80	−0.16(8)	0.9998	0.6	−2.64(8)	0.9996	0.4	−1.46(9)	0.9999	0.4
Aluminosilicates									
Ca3627	−1.6(1)	0.9998	0.7	−5.1(3)	0.9991	3	−2.6(2)	0.9996	1.0
Ca4412	−2.0(1)	0.9995	1.8	−5.5(4)	0.9984	6	−3.0(3)	0.9992	3.0
Ca7611	−1.59(6)	0.99991	0.3	−4.75(6)	0.9999	0.3	−3.23(5)	0.99997	0.09
$NaAlSi_3O_8$	−3.1(3)	0.9997	0.5	−5.5(2)	0.9998	0.3	−5.1(2)	0.9998	0.4
Borosilicates									
Pyrex	1.0(4)	0.9931	9.6	−4.5(3)	0.9959	5.7	0.4(5)	0.9940	8.3
BB	0.11(9)	0.9998	0.4	−2.2(2)	0.9995	0.9	−1.1(1)	0.9997	0.5
BNC	0.005(51)	0.9999	0.3	−2.99(9)	0.9998	0.5	−1.16(3)	0.99998	0.06
E	−1.4(3)	0.99997	0.06	−4.8(1)	0.9997	0.8	−3.04(8)	0.99992	0.2
Titania-Silica									
$24Na_2O-76SiO_2$	0.71(8)	0.9997	0.3	−1.16(6)	0.9999	0.1	−0.25(7)	0.9999	0.2
$23Na_2O-1TiO_2-76SiO_2$	0.55(8)	0.9998	0.3	−1.56(6)	0.9999	0.1	−0.54(7)	0.9999	0.1
$22Na_2O-2TiO_2-76SiO_2$	0.77(9)	0.9996	0.4	−1.3(1)	0.9997	0.4	−0.2(1)	0.9997	0.3
$19Na_2O-5TiO_2-76SiO_2$	0.5(1)	0.9997	0.4	−1.80(8)	0.9999	0.2	−0.6(1)	0.9998	0.2
$17Na_2O-8TiO_2-75SiO_2$	1.07(8)	0.9999	0.2	−1.6(1)	0.9999	0.2	0.0002(103)	0.99992	0.1
$15Na_2O-9TiO_2-76SiO_2$	0.59(4)	0.99998	0.03	−2.10(9)	0.99992	0.1	−0.61(5)	0.99999	0.02
Chalcogenides									
$Se_{90}Te_{10}$	−1.5(1)	0.9964	7.6	−3.35(5)	0.9997	0.7	−1.9(1)	0.9977	5.0
$Se_{95}Te_5$	−1.0(1)	0.9978	6.2	−3.20(6)	0.9996	1	−1.5(1)	0.9986	4.0
Se	−1.3(2)	0.9968	6.3	−3.7(2)	0.9985	3	−2.1(2)	0.9976	5.0
As_2Se_3	−4.1(2)	0.9995	0.6	−8.0(2)	0.9994	0.9	−6.4(3)	0.9994	0.7

[1] L. Berthier and G. Biroli, Rev. Mod. Phys. **83**, 587 (2011).
[2] J. C. Mauro and E. D. Zanotto, Int. J. Appl. Glass Sci. **5**, 313 (2014).
[3] J. C. Mauro, Front. Mater. **1**, 20 (2014).
[4] A. C. P. Rosa Jr., C. Cruz, W. S. Santana, and M. A. Moret, Phys. Rev. E **100**, 022139 (2019).
[5] A. C. P. Rosa, C. Cruz, W. S. Santana, E. Brito, and M. A. Moret, Phys. Rev. E **101**, 042131 (2020).
[6] Q. Zheng and J. C. Mauro, J. Am. Ceram. Soc. **100**, 6 (2017).
[7] D. G. Truhlar and A. Kohen, Proc. Natl. Acad. Sci. USA **98**, 848 (2001).
[8] A. Rosa, P. Vaveliuk, K. C. Mundim, and M. Moret, Physica A **450**, 317 (2016).
[9] V. H. Carvalho-Silva, N. D. Coutinho, and V. Aquilanti, Front. Chem. **7**, 380 (2019).
[10] V. H. Carvalho-Silva, N. D. Coutinho, and V. Aquilanti, Molecules **25**, 2098 (2020).
[11] J. Kohout, Molecules **26**, 7162 (2021).
[12] K. M. Emran, I. M. A. Omar, S. T. Arab, and N. Ouerfelli, Sci. Rep. **12**, 6432 (2022).
[13] C. Torregrosa Cabanilles, J. Molina-Mateo, R. Sabater i Serra, J. Meseguer-Dueñas, and J. Gómez Ribelles, J. Non-Cryst. Solids **576**, 121245 (2022).
[14] P. K. Roy and A. Heuer, J. Chem. Phys. **157**, 174506 (2022).
[15] I. Bondarchuk, S. Bondarchuk, A. Vorozhtsov, and A. Zhukov, Molecules **28**, 424 (2023).
[16] J. C. Mauro, Y. Yue, A. J. Ellison, P. K. Gupta, and D. C. Allan, Proc. Natl. Acad. Sci. USA **106**, 19780 (2009).
[17] W. Zhu, M. Marple, M. Lockhart, B. Aitken, and S. Sen, J. Non-Cryst. Solids **495**, 102 (2018).
[18] L. M. C. Janssen, Front. Phys. **6**, 97 (2018).
[19] K. G. Sturm, Ceramics **4**, 302 (2021).
[20] G. Urbain, Y. Bottinga, and P. Richet, Geochim. Cosmochim. Acta **46**, 1061 (1982).
[21] A. Sipp, Y. Bottinga, and P. Richet, J. Non-Cryst. Solids **288**, 166 (2001).
[22] D. R. Neuville, Chem. Geol. **229**, 28 (2006).
[23] S. P. Jaccani, O. Gulbiten, D. C. Allan, J. C. Mauro, and L. Huang, Phys. Rev. B **96**, 224201 (2017).

[24] A. Sipp, D. R. Neuville, and P. Richet, J. Non-Cryst. Solids **211**, 281 (1997).
[25] G. Gruener, P. Odier, D. D. S. Meneses, P. Florian, and P. Richet, Phys. Rev. B **64**, 024206 (2001).
[26] M. Liška, P. Šimurka, J. Antalík, and P. Perichta, Chem. Geol. **128**, 199 (1996).
[27] P. Koštál and J. Málek, J. Non-Cryst. Solids **356**, 2803 (2010).
[28] P. Koštál and J. Málek, Pure Appl. Chem. **87**, 239 (2015).
[29] J. Barták, P. Koštál, D. Valdés, J. Málek, T. Wieduwilt, J. Kobelke, and M. A. Schmidt, J. Non-Cryst. Solids **511**, 100 (2019).
[30] X.-Y. Gao, C.-Y. Ong, C.-S. Lee, C.-T. Yip, H.-Y. Deng, and C.-H. Lam, Phys. Rev. B **107**, 174206 (2023).
[31] R. S. Welch, E. D. Zanotto, C. J. Wilkinson, D. R. Cassar, M. Montazerian, and J. C. Mauro, Acta Mater. **254**, 118994 (2023).
[32] R. C. D. Passos, D. R. Cassar, and E. D. Zanotto, Ceramics Int. **48**, 13440 (2022).
[33] G. W. Scherer, J. Am. Ceram. Soc. **75**, 1060 (1992).
[34] I. Avramov and A. Milchev, J. Non-Cryst. Solids **104**, 253 (1988).
[35] S. Bellavia, S. Gratton, and E. Riccietti, Numer. Math. **140**, 791 (2018).